Published in final edited form as:
J Phys Chem A. 2011 March 24; 115(11): 2087–2095. doi:10.1021/jp104177q.

Density functional calculation of the structure and electronic properties of Cu_nO_n (n=1-8) clusters

Gyun-Tack Bae, **Barry Dellinger**, and **Randall W. Hall**
Department of Chemistry, Louisiana State University, Baton Rouge, LA 70808

Abstract

Ab initio simulations and calculations were used to study the structures and stabilities of copper oxide clusters, Cu_nO_n (*n*=1-8). The lowest energy structures of neutral and charged copper oxide clusters were determined using primarily the B3LYP/LANL2DZ model chemistry. For $n \geq 4$, the clusters are nonplanar. Selected electronic properties including atomization energies, ionization energies, electron affinities, and Bader charges were calculated and examined as a function of *n*.

Introduction

There is a growing recognition that catalytic metal oxide nanoclusters can play a key role in various environmental processes,[1,2] and it has been suggested that metal oxide clusters contribute to health hazards associated with airborne fine particles.[3–6] Polychlorinated dibenzo-p-dioxins and dibenzofurans (PCDD/F) can be formed in almost any thermal system if there are sources of carbon, chlorine, and transition metals to catalyze chlorination and condensation reactions.[7] Copper and iron oxide nanostructured particles have been shown to be particularly effective catalysts for the formation of PCDD/F and other pollutants at relatively low temperatures as gases exit a combustor.[8] Environmentally persistent free radicals (EPFRs) form over copper and iron oxide-containing nanoparticles, and these EPFRs have been shown to be intermediates in the formation of PCDD/F and be a possible cause of the observed health impacts of airborne fine particles.[9–13] It is thought the EPFRs are formed by an electron transfer from a physisorbed molecular species to the metal atom in a metal oxide cluster. For this reason, studies that determine the geometric structures and charge distributions in neutral and anionic metal oxide clusters are needed.

There are relatively few experimental and theoretical studies of how copper and iron oxide clusters catalyze or mediate the formation of pollutants in combustion systems or the environment. Estimates of the relevant cluster sizes range from a micrometer down to just a few metal atoms; Therefore, this work studies the structures and energetics of small copper oxide clusters as a first step towards understanding the interactions between metal oxides and free radicals.

Experimental[14–24] and computational[21,25–39] studies exist for some small copper oxide clusters. Three isomers have been suggested as possible structures for CuO_2:[20] bent CuOO (bent, C_s), linear OCuO, and C_{2v} OCuO. Evidence has been found for both bent CuOO[18,27,36,37] and linear OCuO.[20,23,32] Vibrational frequencies have been calculated[23] for CuO_3, $OCuO_2^-$, and $Cu(O_3)^-$ clusters. Recently, the structures of CuO_4, CuO_5,[38] and neutral and negatively charged CuO_6 clusters[40] were determined using plane-wave density functional theory. In addition, Cu_2O_n (n=1-4) clusters have been studied using anion

Correspondence to: Randall W. Hall.

photoelectron spectroscopy and density functional calculations.[21,39] In this paper, we investigate the electronic and geometric structures of neutral and charged copper oxide clusters $(CuO)_n$ n=1-8.

Methods

We evaluated several basis sets as candidates for our studies: 6-31G**,[41–43]6-31++G**,[41,44–48] 6-311G**,[47,49–51] 6-311++G**,[46,47] LANL2DZ,[52–54] and DGDZVP.[55,56] Density functional theory using the B3LYP functional was used for the majority of the calculations; the M06 and BHandHLYP functionals were used as a check on the reliability of the B3LYP functional. All calculations were restricted so that the spin states were pure and did not contain any spin contamination.

The study of atomic and molecular clusters can be hindered by the existence of multiple isomers for a given size cluster. Without an *a priori* knowledge of the global energy minima, the use of computer simulation methods, such as simulated annealing, often allow the determination of global minima. For this reason, we performed *ab initio* simulated annealing Monte Carlo (MC) simulations to locate stable geometric structures for the smaller ($n_{Cu} \leq 4$) clusters. Standard single particle MC moves were used and instead of a classical force field Gaussian 03[57] was used to calculate the energy using the B3LYP/6-31G** model chemistry. This 6-31G** basis was chosen as a good compromise between basis set accuracy and computational effort. A MC "pass" corresponded to an attempt to move each atom in the three cartesian directions by up to 0.2 A in each direction. The Metropolis algorithm[58] was used to accept or reject proposed moves. The temperature was linearly decreased from 2000 K to 300 K for up to 500 MC passes. As in standard MC simulations, the total number of passes was dependent on the size of the cluster and the number of passes required before the energy of the cluster equilibrated. For each cluster size, several different initial geometries were used in order to locate with confidence the global minimum. For example, three different starting geometries were used to simulate the Cu_4O_4 cluster, all generated by adding a Cu-O unit to the minimum energy neutral Cu_3O_3 cluster (two added equatorially and one added axially). All three geometries converged to the same final Cu_4O_4 geometry.

The final geometry from each MC simulation was optimized using standard *ab initio* methods with the GAMESS[59] quantum chemistry package using the B3LYP/LANL2DZ model chemistry, d-functions were represented with 6 cartesian functions, the default for GAMESS. The smaller clusters were then used as starting points to look for the global minimum geometries for larger clusters where the Monte Carlo procedure was not computationally feasible. For the larger clusters, standard *ab initio* optimizations were performed using several starting geometries for each cluster size. This procedure was chosen as the option when computational resources did not allow for MC simulations since, consistent with the MC procedure, it did use different initial geometries. In effect, we followed the standard protocol for studying clusters using *ab initio* methods. An alternative would be to use smaller basis sets that would allow larger clusters to be simulated; however, concerns about the accuracy of the smaller basis sets led us to avoid this option.

For the GAMESS optimizations, we used the B3LYP (Becke's 3-parameter exchange functional with Lee-Yang-Parr correlation energy functional) [60–62] version of DFT in combination with a variety of basis sets. Although there are well known deficiencies with the B3LYP functional (particularly for excited states[63]), there are plenty of studies of transition metal clusters (neutral and charged) for which the B3LYP/LANL2DZ basis set has been used successfully.[64–68] For TiO_2 and TiO, Qu and Kroes[64] found (in comparison to experiment) vibrational frequencies accurate to about 60 wavenumbers, ionization energies accurate to 0.2 eV, and electron affinities accurate to 0.2 eV. For neutral and

charged gold atoms, Okumura, Kitagawa, Haruta, and Yamaguchi found[66] ionization energies and electron affinities accurate to 0.2 eV. For the neutral clusters, singlet and triplet states were optimized for *n* even and doublet and quartet states were optimized for *n* odd. For the neutral clusters with triplet/quartet lowest energy structures, single point calculations of quintet/sextet states at the geometries of the triplet/quartet were used as a check of the lowest energy spin state. The spin states examined for the anion and cation were dependent on the spin state of the neutral. For the anions, the two spin states examined corresponded to the addition of an electron to an unfilled orbital and to the addition of an electron to a half-filled orbital (where applicable). For the cations, two spin states were also examined and corresponded to the removal of an electron from a half-filled orbital (were applicable) and a doubly filled orbital. For the neutral clusters, all isomers and spin states were optimized using the M06/LANL2DZ and BHandHLYP/LANL2DZ model chemistries. The lowest energy geometries and spin states were the same for all model chemistries.

Bader charge densities were calculated using the Firefly QC software package[69] to generate cube files, which where then used by the Texas Bader software package[70] to calculate the charge densities. No geometric symmetry was enforced in the calculations in order to allow for symmetry-breaking to lower the total energy. In selected cases, a higher symmetry was used, but in these cases the resulting optimized structure was found to be higher in energy than the structure with no symmetry and to be a transition state (based on vibrational frequencies).

Results and Discussion

We evaluated several basis sets as candidates for our studies: 6-31G**,[41–43] 6-31++G**,[41,44–48] 6-311G**,[47,49–51] 6-311++G**,[46,47] LANL2DZ,[52–54] and DGDZVP.[55,56] Monte Carlo calculations followed by GAMESS optimization found the lowest energy clusters for Cu_2O_n ($n = 1 – 4$) shown in Figure 1. For Cu_2O_3 and Cu_2O_4, different isomers were found depending on basis set (Cu_2O_3-a: 6-31G**; Cu_2O_3-b: 6-31++G**, 6-311G**, 6-311++G**, LANL2DZ and DGDZVP; Cu_2O_4-a: 6-31++G**, 6-311++G**, LANL2DZ and DGDZVP; Cu_2O_4-b: 6-31G** and 6-311G**). A comparison of calculated (adiabatic) and measured electron affinities[21] is shown in Table 1. For comparison, the table also presents results using a customized basis set with diffuse orbitals (WWD).[21] The 6-31++G**, 6-311++G**, DGDZVP, and the WWD basis sets use diffuse orbitals, which are expected to be more accurate for anions. The best agreement with experimental electron affinities was found with the LANL2DZ basis set, despite its lack of diffuse orbitals. Based on the agreement with experimental electron affinities and the success of this model chemistry in previous studies,[64–68] the LANL2DZ basis set was used in the remainder of this work.

The optimized structures of neutral and charged $(CuO)_n$ clusters with n=1-8 clusters are shown in Figure 2, Figure 3, and Figure 4. With the exception of Cu_2O_2, the displayed geometries were between 0.6 and 2.0 eV more stable than any other isomer studied in this work. The Bader charges and spin densities are shown for the neutral clusters in Figure 2. The spin states, spin densities, and the copper- and oxygen-centered charges are displayed for the neutral clusters in Table 2. Detailed Bader charges are given in Table 3. The bondlengths are given in Table 6 and Table 7. The calculated bond lengths for CuO^- and CuO are 1.74Å and 1.81Å and compare well with the measured values of 1.67Å and 1.72Å.[24]

The structure of the lowest energy Cu_2O_2 cluster is a rhombus. The spin states of optimized structures are singlet, doublet, and doublet for the neutral, cation and anion clusters, respectively. Wang et al.[21] and Dai et al.[39] have suggested minimum energy structures for Cu_2O_2 based on *ab initio* calculations and/or experimental measurements. Wang et al.

suggest the structure is a rhombus while Dai et al. suggest the structure is linear or near linear. Our optimized linear Cu_2O_2 cluster structure is about 0.02eV higher in total energy than our rhombus structure. While this is a small energy difference, the three density functionals (B3LYP, M06, and BHandHLYP) used in this study all agreed that rhombus is the lowest energy structure. The rhombic structure of Wang et al. has a Cu-O bond length of 1.78Å and a Cu-O-Cu bond angle of 80°. Our calculations give a Cu-O bond length of ≈ 1.86Å and a Cu-O-Cu bond angle of ≈ 82°. The present work supports the rhombic structure as the lowest energy structure for Cu_2O_2.

Our calculations find Cu_3O_3 clusters to be nearly planar. The spin states of optimized structures are quartet, singlet, and triplet for the neutral, cation and anion clusters, respectively. The average Cu-O-Cu bond angles are 119.9° (cation), 98.1° (neutral), and 94.2° (anion). The calculated Cu-O bond lengths are 1.80Å (cation), 1.90Å (neutral) and 1.85Å (anion). The Cu_4O_4 cluster is the first nonplanar structure found for Cu_nO_n and consists of 2 copper atoms above and below the plane of a Cu_2O_4 unit. Notably, there is an O-O bond in this structure. The addition of the O-O unit helps form a nonplanar 7-membered ring, as well as increasing the O-Cu-O bond angles to ≈ 161°, closer to the 180° angle found in the bulk. A similar structure is found for the cation cluster, while the anion cluster is planar. The spin states of the optimized structures are triplet (neutral) and quartet (cation and anion.) The Cu-O bond lengths are 1.94Å (cation), 1.94Å (neutral), and 1.83Å (anion).

The Cu_5O_5 clusters consist of fused 6-membered (Cu_3O_3) and 7-membered (Cu_3O_4) rings sharing a O-Cu-O edge. The angle between the rings is ≈113°. In these clusters, there is one O-O bond. The spin states of the optimized structures are quartet(neutral) and triplet(cation and anion). Cu_6O_6 clusters have cage structures. The spin states of the optimized structures are triplet(neutral), quartet(cation) and doublet(anion). Cu_7O_7 clusters exhibit another type of fused structure, with three rings sharing a common edge. Similar to the Cu_5O_5 clusters the rings are 6- and 7-membered. There are two O-O bonds in these structures. We were unable to optimize the $^3Cu_7O_7^+$ due to severe spin-contamination issues. The spin states of optimized structures are quartet(neutral) and triplet(anion). Cu_8O_8 is formed by adding a Cu_2O_2 group to the edge of the Cu_6O_6 cluster. The spin states of the optimized clusters are triplet (neutral), quartet (cation and anion.)

Table 5 displays the spin state, the adiabatic ionization energies, the electron affinities, and the atomization energies per CuO group. The bond lengths are given in Table 6 and Table 7. The atomization energies per atom have been calculated from

$$E_a=[n\,E(Cu)+n\,E(O)-E(Cu_nO_n)]/2n \quad (1)$$

Figure 5 displays the atomization energy per atom, E_a, as a function of the number of copper atoms in the cluster. This energy rises rapidly from n = 1 to n = 5 and appears to be converging at about 2.5 eV. The second difference in energies is defined by

$$\Delta^2E(n)=[E(n+1)-E(n)]-[E(n)-E(n-1)] \quad (2)$$

and is often used to identify so-called “magic clusters”, clusters that are particularly stable. The second difference is plotted in Figure 6. For the neutral clusters, there is an odd-even alternation in the values of $\Delta^2E(n)$ with Cu_5O_5 and Cu_7O_7 (and possibly Cu_3O_3) appearing

to be particularly stable. The trends for the anionic clusters is similar to the trends for neutral clusters with the exception of $n = 7$, where the neutral cluster is relatively quite stable while the anionic cluster is relatively less stable (and not a magic cluster). There is a change in coordination of one of the copper atoms in the $n = 8$ cluster from 4-coordinate to 2-coordinate in oxygen upon formation of the anion (copper atom five in Figure 5). This change in geometry may account for the different behavior in the value of $\Delta^2E(n)$ for the $n = 7$ neutral and anion. The cationic clusters have the opposite behavior in that magic neutral and anionic clusters have correspondingly unstable cationic clusters for $n = 2 – 5$.

Of particular interest in this work are the charge and spin density differences between neutral and anionic clusters as these differences may lead to reactivity differences between different clusters and EPFR precursors. The average values for these quantities on the copper and oxygen atoms in the neutral clusters are displayed in Table 2 and the values for all atoms in all the clusters are displayed in Table 3. These quantities may correlate with the reactivity of these clusters towards EPFRs. As should be expected, the unpaired electrons reside primarily on the oxygen atoms. For $n \geq 3$, there is a clear alternation in the oxygen spin density indicating that extra unpaired electron for the quartet state (n even) clusters resides mainly on the oxygen atoms. With the exception of $n = 5$ and $n = 6$, the most and least stable clusters according to the second difference in energies, there is roughly 0.5e of unpaired electron density on the copper atoms. The magic $n = 5$ cluster has an extra 0.5e on the copper atoms, as compared to the other odd numbered clusters with $n \geq 3$. This shift of about one half of an electron is also seen for $n = 6$. The charge densities seem to be converging to values consist with the transfer of approximately 0.7 electrons from the copper atoms to the oxygen atoms. Reactions of these clusters with persistent free radicals are expected to be facilitated by the transfer of electron density from the free radical to the metal oxide cluster. Therefore, we calculated the difference in charge density between the anion and neutral clusters for each copper atom as a measure of the likelihood that a particular atom may be a reaction site for a free radical. These differences are displayed in Table 4. For $n \geq 4$, there are substantial differences in the change in the charge between copper atoms in a cluster. For $n = 4$, $n = 5$, and 7 the copper atoms in the most highly strained (smallest) ring in the neutral accept the largest portion of the negative charge. For $n = 5$, the central copper atom (atom 5 in Figure 2) does not accept any of the negative charge even though it is a member of the most strained ring. For $n = 6$, all copper atoms except the 4-coordinated atom (atom 6 in Figure 2) accept roughly an equal amount of charge. In the $n = 8$ cluster, there is a change in geometry from neutral to anion, resulting in the conversion of a 4-coordinate copper atom to a 2-coordinate oxygen atom (atom 5 in Figure 2). It is this copper atom that accepts the majority of the added charge.

The local geometries around Cu and O atoms in bulk CuO are roughly square planar and tetrahedral, respectively. An analysis of the local bond angles shown in Table 8 in the copper oxide clusters gives insight as to the particular stabilities of the odd number clusters ($n = 3$, 5, and 7). The Cu-O-Cu angles are relatively close to tetrahedral values and correlate reasonably well with the stability suggested by the second energy differences. No correlation was found between O-Cu-O angles (which are quite distorted from the 90 and 180 angles that characterize a square planar geometry) and stability.

Figure 7 displays the adiabatic ionization energies and electron affinities. The ionization energy of CuO is in good agreement with experiment (calculated 9.28 eV versus experimental 9.41 eV[71]). These quantities seem to be converging for $n \geq 3$. There is a slight even-odd oscillation in ionization energies, but overall little structure to either quantity except for the electron affinity of Cu_7O_7.

Conclusions

The electronic and structural properties of small copper oxide clusters have been studied using density functional theory and several basis sets. The LANL2DZ basis set gave the best agreement with existing experimental work and therefore was used to study Cu_nO_n clusters. The M06 and BHandHLYP functionals gave the same structures and spin states as the B3LYP functional for the neutral clusters. It was found that the clusters are planar for up to $n = 3$ and then become nonplanar. Clusters with an odd number of copper atoms were more stable than clusters containing an even number of copper atoms, possibly due to less strain in the Cu-O-Cu bond angles.

The Bader spin and charge densities show relatively constant spin densities on the copper atoms and alternating (depending on spin state) densities on the oxygen atoms. The magic cluster Cu_5O_5 is the most "copper-centered" radical with the most unpaired electron density on the copper atoms. Stability appears to be correlated with the deviation of the Cu-O-Cu bond angles in a cluster from a tetrahedral geometry; the less distorted structures are the most stable. The odd numbered clusters found in this work have the largest "rings" of copper and oxygen atoms, which allows the Cu-O-Cu angles adopt angles closer to ideal tetrahedral geometries.

Analysis of the differences in charge density between neutral and anionic species show copper atoms in the most strained rings most likely to accept electron density when the neutral is converted to an anion. There are clearly differences between the charge densities on individual copper atoms in a cluster and between the ability (measured by the change in charge density on a given copper atom) of a copper atom to add electron density when the anion is formed. These differences are likely to correlate with the reactivity of different sites on a cluster and should affect the preference for the way in which different clusters react with free radicals and EPFR precursors. We expect that the copper atoms that accept the largest fraction of an electron when forming the anion will be the sites at which free radicals will react.

Acknowledgments

This work was supported by NSF CBET-0625548 and CTS-0404314 and NIEHS 1P42ES013648-01A2 grants and computational facilities at Louisiana State University and the Louisiana Optical Network Initiative.

References

1. Lighty JS, Veranth JM, Sarofim AF. Journal of the Air and Waste Management Association. 2000; 50:1565–1618. [PubMed: 11055157]
2. Linak WP, Wendt JOL. Fuel Processing Technology. 1994; 39:173–198.
3. Pope CA, Burnett RT, Thun MJ, Calle EE, Krewski D, Ito K, Thurston GD. JAMA. 2002; 287:1132–41. [PubMed: 11879110]
4. Delfino R, Gong H, Linn W, Pellizzari E, Hu Y. Environmental Health Perspectives. 2003; 111:647–656. [PubMed: 12676630]
5. Donaldson K, Li X, MacNee W. Journal of Aerosol Science. 1998; 29:553–560.
6. Air Quality Criteria for Particulate Matter 1-3, EPA/600/P-95/001. 1996.
7. Thomas VM, Spiro TG. Environ Sci Technol. 1996; 30:A82–A85.
8. Ryan S, Wikstrom E, Gullett BK, Touati A. Organohalogen Compounds. 2004; 66:1119–1125.
9. Dellinger B, Pyror W, Cueto R, Squadrito G, Hedge V, Deutsch W. Chem Res Toxicol. 2001; 14:1371–1377. [PubMed: 11599928]
10. Dellinger B, Pryor W, Cueto R, Squadrito G, Deutsch W. Proceedings of the Combustion Institute. 2000; 28:2675–2681.

11. Shi T, Knaapen A, Begerow J, Birmili W, Borm P, Schins R. Occup Environ Med. 2003; 60:315–321. [PubMed: 12709515]
12. Li N, Sioutas C, Cho A, Schmitz D, Misra C, Sempf J, Wang M, Oberley T, Froines J, Nel A. Environmental Health Perspectives. 2003; 111:455–460. [PubMed: 12676598]
13. Balakrishna S, Lomnicki S, McAvey KM, Cole RB, Dellinger B, Cormier SA. Particle and Fibre Toxicology. 2009; 6:11. [PubMed: 19374750]
14. Ozin G, Mitchell S, Garcia-Prieto J. Journal of the American Chemical Society. 1983; 105:6399–6406.
15. Tevault DE. Journal of Chemical Physics. 1982; 76:2859–2863.
16. Bondybey VE, English JH. Journal of Physical Chemistry. 1984; 88:2247–2250.
17. Howard JA, Sutcliffe R, Mile B. Journal of Physical Chemistry. 1984; 88:4351–4354.
18. Kasai PH, Jones PM. Journal of Physical Chemistry. 1986; 90:4239–4245.
19. Madhavan PV, Newton MD. Journal of Chemical Physics. 1985; 83:2337–2347.
20. Wu HB, Desai SR, Wang LS. Journal of Chemical Physics. 1995; 103:4363–4366.
21. Wang LS, Wu HB, Desai SR, Lou L. Physical Review B. 1996; 53:8028–8031.
22. Wu H, Desai SR, Wang LS. Journal of Physical Chemistry A. 1997; 101:2103–2111.
23. Chertihin GV, Andrews L, Bauschlicher CW. Journal of Physical Chemistry A. 1997; 101:4026–4034.
24. Polak ML, Gilles MK, Ho J, Lineberger WC. Journal of Physical Chemistry. 1991; 95:3460–3463.
25. Igel G, Wedig U, Dolg M, Fuentealba P, Preuss H, Stoll H, Frey R. Journal of Chemical Physics. 1984; 81:2737–2740.
26. Bagus PS, Nelin CJ, Bauschlicher CW. Journal of Chemical Physics. 1983; 79:2975–2981.
27. Hrusak J, Koch W, Schwarz H. Journal of Chemical Physics. 1994; 101:3898–3905.
28. Ha TK, Nguyen MT. Journal of Physical Chemistry. 1985; 89:5569–5570.
29. Den Boer DHW, Kaleveld EW. Chemical Physics Letters. 1980; 69:389–395.
30. Mochizuki Y, Tanaka K, Kashiwagi H. Chemical Physics. 1991; 151:11–20.
31. Barone V, Adamo C. Journal of Physical Chemistry. 1996; 100:2094–2099.
32. Deng K, Yang JL, Yuan LF, Zhu QS. Journal of Chemical Physics. 1999; 111:1477–1482.
33. Cao Z, Sola M, Xian H, Duran M, Zhang Q. International Journal of Quantum Chemistry. 2001; 81:162–168.
34. Pouillon Y, Massobrio C. Chemical Physics Letters. 2002; 356:469–475.
35. Pouillon Y, Massobrio C. Applied Surface Science. 2004; 226:306–312.
36. Mattar SM, Ozin GA. Journal of Physical Chemistry. 1988; 92:3511–3518.
37. Bauschlicher CW, Langhoff SR, Partridge H, Sodupe M. Journal of Physical Chemistry. 1993; 97:856–859.
38. Massobrio C, Pouillon Y. Journal of Chemical Physics. 2003; 119:8305–8310.
39. Dai B, Tian L, Yang JL. Journal of Chemical Physics. 2004; 120:2746–2751. [PubMed: 15268419]
40. Pouillon Y, Massobrio C. Chemical Physics Letters. 2002; 356 PII S0009–2614(02)00385–8.
41. Francl MM, Pietro WJ, Hehre WJ, Binkley JS, Gordon MS, Defrees DJ, Pople JA. Journal of Chemical Physics. 1982; 77:3654–3665.
42. Rassolov VA, Pople JA, Ratner MA, Windus TL. Journal of Chemical Physics. 1998; 109:1223–1229.
43. Harihara P, Pople JA. Theoretica Chimica Acta. 1973; 28:213–222.
44. Hehre WJ, Ditchfie R, Pople JA. Journal of Chemical Physics. 1972; 56:2257–2261.
45. Dill JD, Pople JA. Journal of Chemical Physics. 1975; 62:2921–2923.
46. Clark T, Chandrasekhar J, Spitznagel GW, Schleyer PvR. Journal of Computational Chemistry. 1983; 4:294–301.
47. Krishnan R, Binkley JS, Seeger R, Pople JA. Journal of Chemical Physics. 1980; 72:650–654.
48. Gill PMW, Johnson BG, Pople JA, Frisch MJ. Chemical Physics Letters. 1992; 197:499–505.

49. Blaudeau JP, McGrath MP, Curtiss LA, Radom L. Journal of Chemical Physics. 1997; 107:5016–5021.
50. Curtiss LA, McGrath MP, Blaudeau JP, Davis NE, Binning RC, Radom L. Journal of Chemical Physics. 1995; 103:6104–6113.
51. Glukhovtsev MN, Pross A, McGrath MP, Radom L. Journal of Chemical Physics. 1995; 103:1878–1885.
52. Hay PJ, Wadt WR. Journal of Chemical Physics. 1985; 82:270–283.
53. Wadt WR, Hay PJ. Journal of Chemical Physics. 1985; 82:284–298.
54. Hay PJ, Wadt WR. Journal of Chemical Physics. 1985; 82:299–310.
55. Godbout N, Salahub DR, Andzelm J, Wimmer E. Canadian Journal of Chemistry-Revue Canadienne De Chimie. 1992; 70:560–571.
56. Sosa C, Andzelm J, Elkin BC, Wimmer E, Dobbs KD, Dixon DA. Journal of Physical Chemistry. 1992; 96:6630–6636.
57. Frisch, MJ., et al. Gaussian 98 Revision A 11.4. Gaussian, Inc.; Pittsburgh PA: 2002.
58. Kalos, MH.; Whitlock, PA. Monte Carlo methods Vol 1 basics. Wiley-Interscience; New York, NY, USA: 1986.
59. Schmidt M, Baldridge K, Boatz J, Elbert S, Gordon M, Jensen J, Koseki S, Matsunaga N, Nguyen K, SJ S, Windus T, Dupuis M, Montgomery J. GAMESS VERSION = 24 MAR 2007 (R3). 1993
60. Lee CT, Yang WT, Parr RG. Physical Review B. 1988; 37:785–789.
61. Becke AD. Journal of Chemical Physics. 1993; 98:1372–1377.
62. Stephens PJ, Devlin FJ, Chabalowski CF, Frisch MJ. Journal of Physical Chemistry. 1994; 98:11623–11627.
63. GuÌĹell M, Luis JM, RodriÌąguez-Santiago L, Sodupe M, SolaÌĂ M. The Journal of Physical Chemistry A. 2009; 113:1308–1317. [PubMed: 19146445]
64. Qu, Zw; Kroes, GJ. The Journal of Physical Chemistry B. 2006; 110:8998–9007. [PubMed: 16671707]
65. Dai B, Deng K, Yang J. Chemical Physics Letters. 2002; 364:188–195.
66. Okumura M, Kitagawa Y, Haruta M, Yamaguchi K. Chemical Physics Letters. 2001; 346:163–168.
67. Mukhopadhyay S, Gowtham S, Pandey R, Costales A. Journal of Molecular Structure: THEOCHEM. 2010; 948:31–35.
68. David Jeba Singh DM, Pradeep T, Thirumoorthy K, Balasubramanian K. The Journal of Physical Chemistry A. 2010; 114:5445–5452. [PubMed: 20377209]
69. Granovsky, A. Firefly version 7.1.G. [10-Oct-2010]. http://classic.chem.msu.su/gran/firefly/index.html, Online
70. Bader Charge Analysis. [10-Oct-2010]. http://theory.cm.utexas.edu/vtsttools/bader/, Online
71. Metz R, Nicholas C, Ahmed M, Leone S. Journal of Chemical Physics. 2005; 123:114313. [PubMed: 16392565]

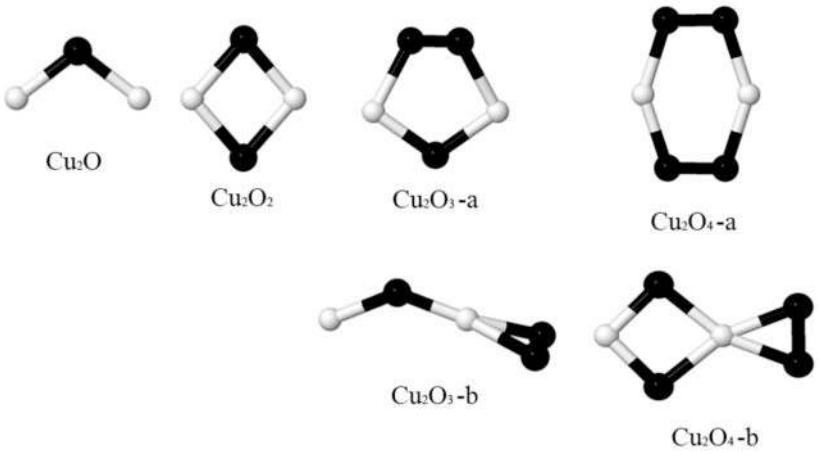

Figure 1.

Lowest energy clusters for Cu_2O_n, n = 1 – 4. Different basis sets give different lowest energy isomers for n = 3 and 4 (Cu_2O_3-a: 6-31G**; Cu_2O_3-b: 6-31++G**, 6-311G**, 6-311++G**, LANL2DZ and DGDZVP; Cu_2O_4-a: 6-31++G**, 6-311++G**, LANL2DZ and DGDZVP; Cu_2O_4-b: 6-31G** and 6-311G**).

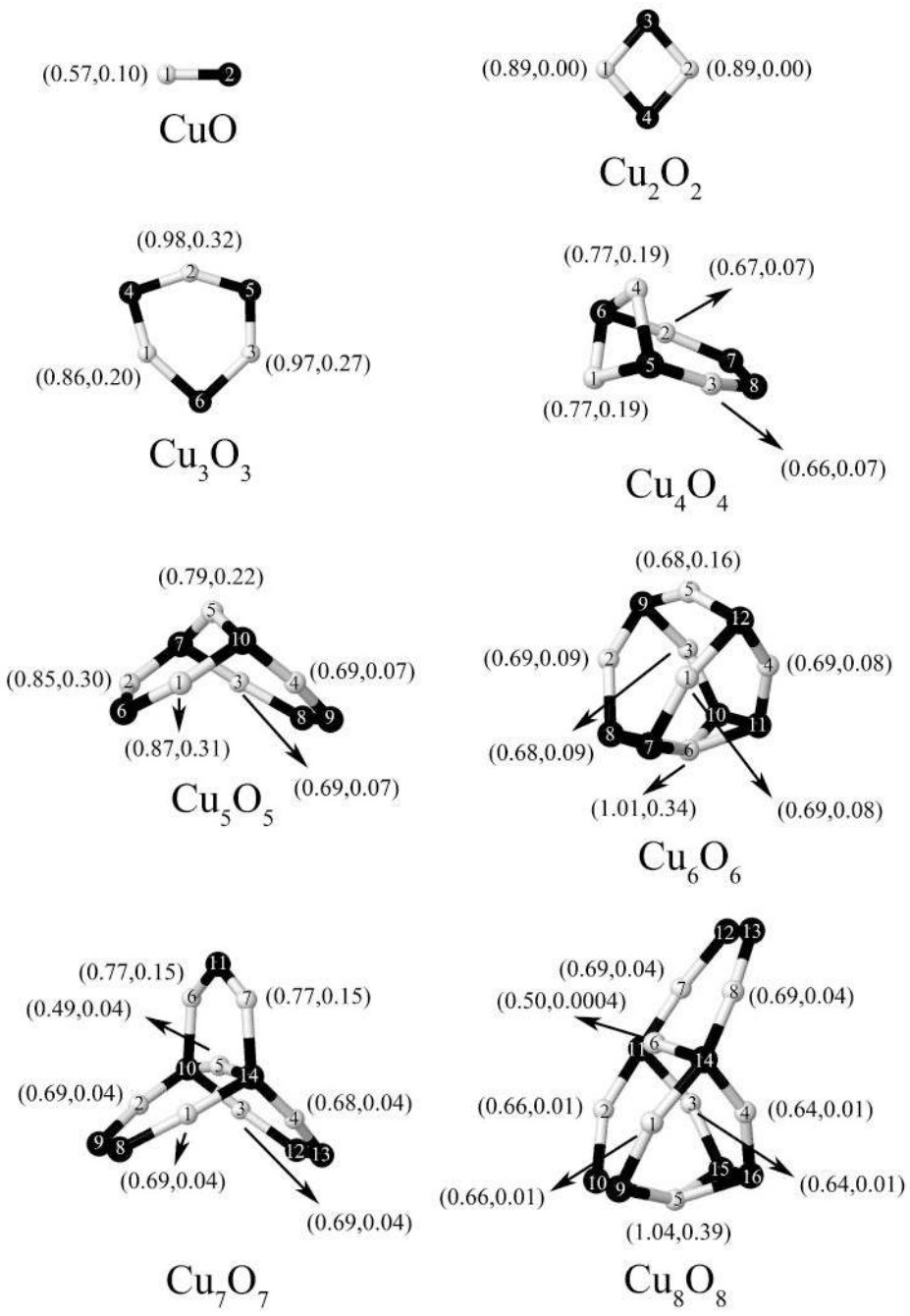

Figure 2.

Optimized structures of neutral $(CuO)_n$ clusters with n=1-8 using the B3LYP/LANL2DZ model chemistry. Bader charges and spin densities for the copper atoms are shown in parentheses. Copper/oxygen atoms are colored white/black.

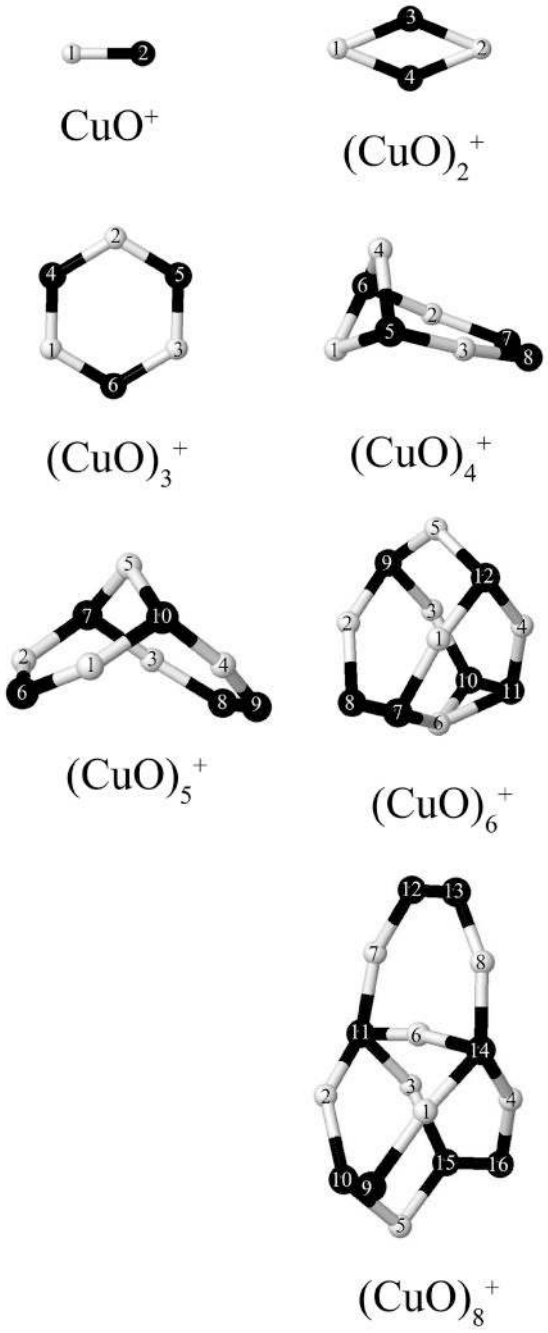

Figure 3.
Optimized structures of cationic $(CuO)_n$ clusters with n=1-8 using the B3LYP/LANL2DZ model chemistry. Copper/oxygen atoms are colored white/black.

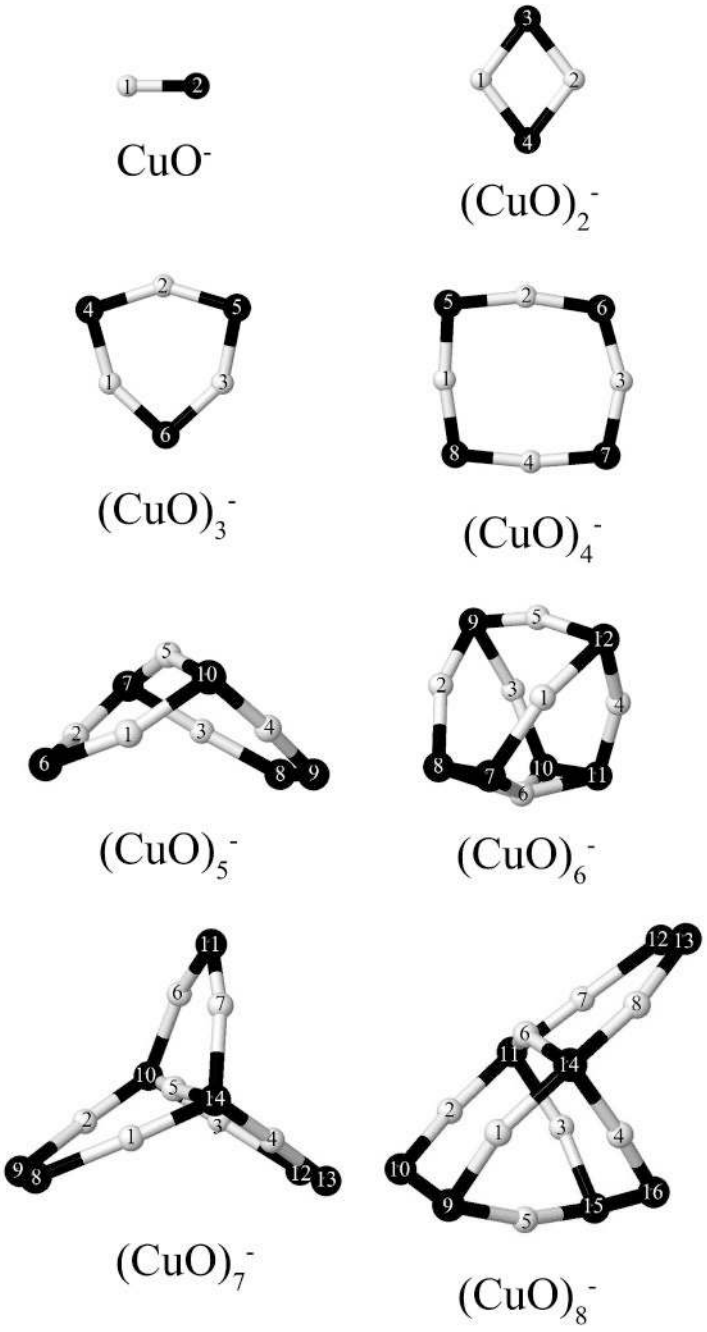

Figure 4.
Optimized structures of anionic $(CuO)_n$ clusters with n=1-8 using the B3LYP/LANL2DZ model chemistry. Copper/oxygen atoms are colored white/black.

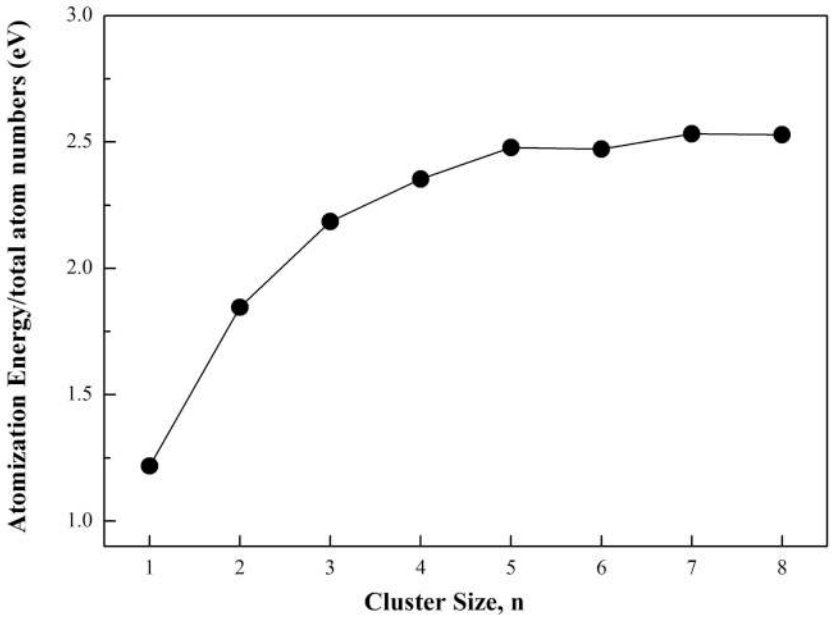

Figure 5.
Atomization energies of neutral $(CuO)_n$ clusters with n=1-8 using the B3LYP/LANL2DZ model chemistry.

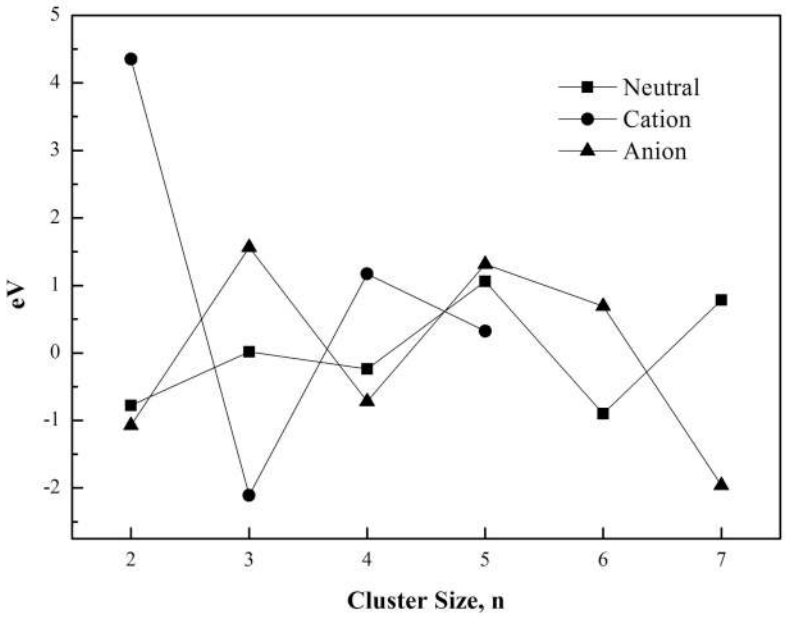

Figure 6.
Second differences of the energy of copper oxide clusters with n=1-8 using the B3LYP/ LANL2DZ model chemistry.

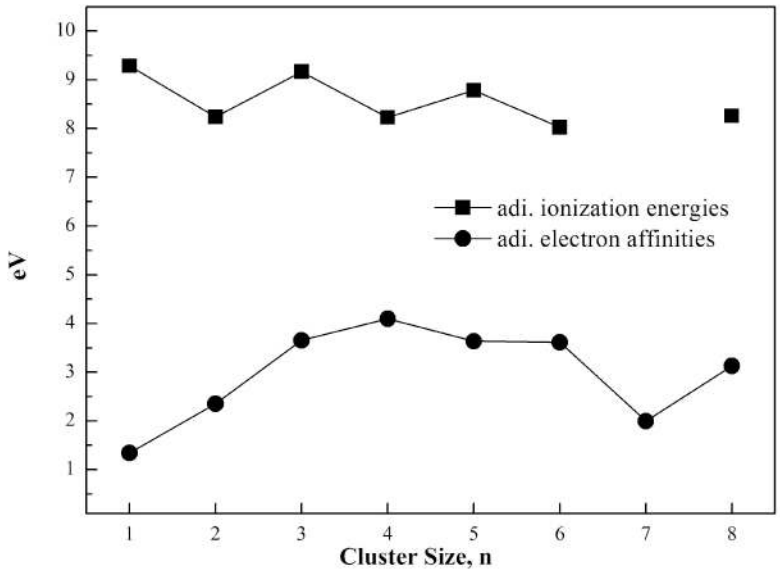

Figure 7.
Calculated adiabatic ionization energies and electron affinities of $(CuO)_n$ clusters with n=1-8 using the B3LYP/LANL2DZ model chemistry.

Table 1

Electron affinity comparing basis sets with experimental data

	Electron Affinities (eV)			
	Cu_2O	Cu_2O_2	Cu_2O_3	Cu_2O_4
6-31G**	0.94	1.41	2.35	3.26
6-31++G**	1.27	2.33	2.65	3.34
6-311G**	0.14	0.89	1.67	2.75
6-311++G**	1.24	1.76	3.09	3.35
LANL2DZ	1.15	2.41	3.25	3.54
DGDZVP	1.15	2.24	3.08	3.31
WWD.[21]	1.10	2.12	3.03	2.94
EXP[21]	1.10	2.46	3.54	3.50

Table 2

Average Bader Charges and spin densities for the neutral $(CuO)_n$ clusters on the copper and oxygen atoms in a cluster as a function of *n* using the B3LYP/LANL2DZ model chemistry

n	Spin Multiplicity	Charge Cu	Charge O	Spin Density Cu	Spin Density O
1	2	+0.57	-0.57	0.10	0.90
2	0	+0.87	-0.89	0	0
3	4	+0.94	-0.93	0.79	2.21
4	3	+0.71	-0.71	0.51	1.49
5	4	+0.78	-0.78	0.98	2.02
6	3	+0.74	-0.74	0.82	1.18
7	4	+0.68	-0.68	0.50	2.50
8	3	+0.69	-0.69	0.50	1.50

Table 3

Bader charges on the copper and oxygen atoms in $(CuO)_n$ (n=1-8) clusters using the B3LYP/LANL2DZ model chemistry. The numbers in parentheses indicate the atom labels from Figure 2

Clusters		qCu(atom number)			qO(atom number)		
CuO	CuO	0.57(1)			-0.57(2)		
	CuO+	0.99(1)			0.01(2)		
	CuO^-	-0.02(1)			-0.99(2)		
Cu_2O_2	Cu_2O_2	0.89(1)	0.89(2)		-0.89(3)	-0.89(4)	
	$Cu_2O_2^+$	0.91(1)	0.91(2)		-0.40(3)	-0.44(4)	
	$Cu_2O_2^-$	0.58(1)	0.58(2)		-1.09(3)	-1.09(4)	
Cu_3O_3	Cu_3O_3	0.86(1)	0.98(2)	0.97(3)	-0.58(4)	-0.91(5)	-1.31(6)
	$Cu_3O_3^+$	1.13(1)	1.11(2)	1.12(3)	-0.79(4)	-0.78(5)	-0.80(6)
	$Cu_3O_3^-$	0.71(1)	0.71(2)	0.70(3)	-1.04(4)	-1.04(5)	-1.03(6)
Cu_4O_4	Cu_4O_4	0.77(1)	0.67(2)		-1.05(5)	-1.05(6)	
		0.66(3)	0.77(4)		-0.41(7)	-0.34(8)	
	$Cu_4O_4^+$	1.13(1)	0.65(2)		-0.96(5)	-0.98(6)	
		0.64(3)	1.19(4)		-0.34(7)	-0.33(8)	
	$Cu_4O_4^-$	0.68(1)	0.64(2)		-1.06(5)	-0.76(6)	
		0.68(3)	0.64(4)		-1.06(7)	-0.76(8)	
Cu_5O_5	Cu_5O_5	0.87(1)	0.85(2)	0.69(3)	-0.96(6)	-1.10(7)	-0.35(8)
		0.69(4)	0.79(5)		-0.39(9)	-1.11(10)	
	$Cu_5O_5^+$	1.00(1)	1.05(2)	0.76(3)	-0.30(6)	-1.18(7)	-0.31(8)
		0.75(4)	0.79(5)		-0.36(9)	-1.20(10)	
	$Cu_5O_5^-$	0.66(1)	0.67(2)	0.62(3)	-0.93(6)	-1.17(7)	-0.42(8)
		0.62(4)	0.55(5)		-0.43(9)	-1.17(10)	
Cu_6O_6	Cu_6O_6	0.69(1)	0.69(2)	0.68(3)	-0.57(7)	-0.58(8)	-1.08(9)

J Phys Chem A. Author manuscript; available in PMC 2012 March 24.

Clusters		qCu(atom number)			qO(atom number)		
		0.69(4)	0.68(5)	1.01(6)	-0.60(10)	-0.56(11)	-1.06(12)
		0.75(1)	0.76(2)	0.76(3)	-0.48(7)	-0.44(8)	-1.08(9)
	$Cu_6O_6^+$	0.75(4)	1.01(5)	0.95(6)	-0.42(10)	-0.48(11)	-1.07(12)
		0.57(1)	0.57(2)	0.56(3)	-0.64(7)	-0.66(8)	-1.12(9)
	$Cu_6O_6^-$	0.57(4)	0.52(5)	1.01(6)	-0.62(10)	-0.64(11)	-1.13(12)
		0.69(1)	0.69(2)	0.69(3)	-0.37(8)	-0.37(9)	-1.21(10)
	Cu_7O_7	0.68(4)	0.49(5)		-0.91(11)	-0.37(12)	
		0.77(6)	0.77(7)		-0.34(13)	-1.19(14)	
Cu_7O_7		0.64(1)	0.63(2)	0.62(3)	-0.86(8)	-0.86(9)	-1.16(10)
	$Cu_7O_7^-$	0.63(4)	0.36(5)		-0.19(11)	-0.86(12)	
		1.11(6)	0.98(7)		-0.86(13)	-1.14(14)	
		0.66(1)	0.66(2)	0.64(3)	-0.59(9)	-0.62(10)	-1.20(11)
	Cu_8O_8	0.64(4)	1.04(5)	0.50(6)	-0.34(12)	-0.38(13)	-1.20(14)
		0.69(7)	0.69(8)		-0.59(15)	-0.61(16)	
		0.70(1)	0.71(2)	0.70(3)	-0.58(9)	-0.64(10)	-1.19(11)
Cu_8O_8	$Cu_8O_8^+$	0.69(4)	0.85(5)	0.48(6)	-0.05(12)	-0.06(13)	-1.09(14)
		0.92(7)	0.91(8)		-0.64(15)	-0.59(16)	
		0.64(1)	0.68(2)	0.61(3)	-0.60(9)	-0.43(10)	-1.21(11)
	$Cu_8O_8^-$	0.65(4)	0.90(5)	0.51(6)	-0.86(12)	-0.86(13)	-1.19(14)
		0.63(7)	0.62(8)	24	-0.63(15)	-0.46(16)	

Table 4

The Change in Bader charges of copper atoms in $(CuO)_n$ (n=1-8) clusters from neutral to anion using the B3LYP/LANL2DZ model chemistry. The numbers in parenthesis label the different copper atoms

Clusters	qCu(atom number)			
CuO	-0.59(1)			
Cu_2O_2	-0.30(1)	-0.31(2)		
Cu_3O_3	-0.15(1)	-0.27(2)	-0.27(3)	
Cu_4O_4	-0.09(1)	-0.03(2)	0.02(3)	-0.13(4)
Cu_5O_5	-0.21(1)	-0.18(2)	-0.07(3)	
	-0.07(4)	-0.24(5)		
Cu_6O_6	-0.12(1)	-0.12(2)	-0.12(3)	
	-0.12(4)	-0.16(5)	0.001(6)	
Cu_7O_7	-0.05(1)	-0.06(2)	-0.07(3)	-0.05(4)
	-0.13(5)	0.34(6)	0.21(7)	
Cu_8O_8	-0.02(1)	0.02(2)	-0.03(3)	0.01(4)
	-0.14(5)	0.01(6)	-0.06(7)	-0.07(8)

Table 5

Spin states, ionization energies (IE), electron affinities (EA), and binding energies (E_b) for Cu_nO_n, n = 1 – 8. Energies are in electron volts and are calculated using the B3LYP/LANL2DZ model chemistry

	Spin State	IE	EA	E_b
CuO	doublet			
CuO+	triplet	9.28	1.35	1.22
CuO^-	singlet			
Cu_2O_2	singlet			
$Cu_2O_2^+$	doublet	8.24	2.35	1.85
$Cu_2O_2^-$	doublet			
Cu_3O_3	quartet			
$Cu_3O_3^+$	singlet	9.16	3.65	2.19
$Cu_3O_3^-$	triplet			
Cu_4O_4	triplet			
$Cu_4O_4^+$	quartet	8.23	4.10	2.35
$Cu_4O_4^-$	quartet			
Cu_5O_5	quartet			
$Cu_5O_5^+$	triplet	8.78	3.64	2.48
$Cu_5O_5^-$	triplet			
Cu_6O_6	triplet			
$Cu_6O_6^+$	quartet	8.02	3.61	2.47
$Cu_6O_6^-$	doublet			
Cu_7O_7	quartet			
$Cu_7O_7^-$	triplet		2.00	2.53
Cu_8O_8	triplet			
$Cu_8O_8^+$	quartet	8.26	3.13	2.53
$Cu_8O_8^-$	doublet			

Table 6

Bond lengths (Å) of Cu-O in $(CuO)_n$ (n=1-8) clusters using the B3LYP/LANL2DZ model chemistry

	Clusters	Distance					
CuO	CuO	d_{1-2}=1.81					
	CuO+	d_{1-2}=2.02					
	CuO^-	d_{1-2}=1.74					
Cu_2O_2	Cu_2O_2	d_{1-3}=1.86	d_{1-4}=1.86	d_{2-3}=1.86	d_{2-4}=1.86		
	$Cu_2O_2^+$	d_{1-3}=2.01	d_{1-4}=2.01	d_{2-3}=2.01	d_{2-4}=2.01		
	$Cu_2O_2^-$	d_{1-3}=1.92	d_{1-4}=1.92	d_{2-3}=1.92	d_{2-4}=1.92		
Cu_3O_3	Cu_3O_3	d_{1-4}=1.83	d_{1-6}=2.06	d_{2-4}=1.81	d_{2-5}=1.83	d_{3-5}=1.83	d_{3-6}=2.03
	$Cu_3O_3^+$	d_{1-4}=1.80	d_{1-6}=1.80	d_{2-4}=1.80	d_{2-5}=1.80	d_{3-5}=1.80	d_{3-6}=1.80
	$Cu_3O_3^-$	d_{1-4}=1.84	d_{1-6}=1.85	d_{2-4}=1.85	d_{2-5}=1.85	d_{3-5}=1.85	d_{3-6}=1.85
Cu_4O_4	Cu_4O_4	d_{1-5}=1.96	d_{1-6}=1.97	d_{2-6}=1.88	d_{2-7}=1.93		
		d_{3-5}=1.88	d_{3-8}=1.93	d_{4-5}=1.97	d_{4-6}=1.96		
	$Cu_4O_4^+$	d_{1-5}=1.94	d_{1-6}=1.93	d_{2-6}=1.86	d_{2-7}=2.00		
		d_{3-5}=1.86	d_{3-8}=2.00	d_{4-5}=1.95	d_{4-6}=1.97		
	$Cu_4O_4^-$	d_{1-5}=1.85	d_{1-8}=1.80	d_{2-5}=1.85	d_{2-6}=1.80		
		d_{3-6}=1.80	d_{3-7}=1.85	d_{4-7}=1.85	d_{4-8}=1.80		
Cu_5O_5	Cu_5O_5	d_{1-6}=1.83	d_{1-10}=1.87	d_{2-6}=1.83	d_{2-7}=1.88	d_{3-7}=1.88	d_{3-8}=1.92
		d_{4-9}=1.92	d_{4-10}=1.87	d_{5-7}=1.90	d_{5-10}=1.90	d_{8-9}=1.40	
	$Cu_5O_5^+$	d_{1-6}=1.87	d_{1-10}=1.87	d_{2-6}=1.80	d_{2-7}=1.88	d_{3-7}=1.88	d_{3-8}=1.87
		d_{4-9}=1.87	d_{4-10}=1.88	d_{5-7}=1.96	d_{5-10}=1.96	d_{8-9}=1.37	
	$Cu_5O_5^-$	d_{1-6}=1.87	d_{1-10}=1.91	d_{2-6}=1.87	d_{2-7}=1.90	d_{3-7}=1.87	d_{3-8}=1.92
		d_{4-9}=1.92	d_{4-10}=1.87	d_{5-7}=1.96	d_{5-10}=1.96	d_{8-9}=1.41	
Cu_6O_6	Cu_6O_6	d_{1-7}=1.94	d_{1-12}=1.90	d_{2-8}=1.94	d_{2-9}=1.90	d_{3-9}=1.90	d_{3-10}=1.94

J Phys Chem A. Author manuscript; available in PMC 2012 March 24.

Clusters	Distance					
$Cu_6O_6^+$	d_{4-11}=1.94	d_{4-12}=1.90	d_{5-9}=1.88	d_{5-12}=1.89	d_{6-7}=2.02	
	d_{6-8}=2.10	d_{6-10}=2.02	d_{6-11}=2.10	d_{7-8}=1.52	d_{10-11}=1.52	
	d_{1-7}=1.96	d_{1-12}=1.89	d_{2-8}=1.95	d_{3-9}=1.89	d_{3-9}=1.89	d_{3-10}=1.94
$Cu_6O_6^-$	d_{4-11}=1.96	d_{4-12}=1.89	d_{5-9}=1.86	d_{5-12}=1.86	d_{6-7}=2.07	
	d_{6-8}=2.24	d_{6-10}=2.28	d_{6-11}=2.06	d_{7-8}=1.46	d_{10-11}=1.46	
	d_{1-7}=1.96	d_{1-12}=1.92	d_{2-8}=1.96	d_{2-9}=1.94	d_{3-9}=1.94	d_{3-10}=1.96
	d_{4-11}=1.96	d_{4-12}=1.92	d_{5-9}=1.91	d_{5-12}=1.92	d_{6-7}=2.01	
	d_{6-8}=2.05	d_{6-10}=2.06	d_{6-11}=2.00	d_{7-8}=1.56	d_{10-11}=1.56	

Table 7

Bond lengths (Å) of Cu-O in $(CuO)_n$ (n=1-8) clusters using the B3LYP/LANL2DZ model chemistry

Clusters		Distance				
Cu_7O_7	Cu_7O_7	d_{1-8}=1.94	d_{1-14}=1.92	d_{2-9}=1.94	d_{2-10}=1.92	d_{3-10}=1.92
		d_{3-12}=1.94	d_{4-13}=1.94	d_{4-14}=1.92	d_{5-10}=1.92	d_{5-14}=1.92
		d_{6-10}=1.98	d_{6-11}=1.88	d_{7-11}=1.88	d_{7-14}=1.98	d_{8-9}=1.40
		d_{12-13}=1.40				
	$Cu_7O_7^-$	d_{1-8}=2.19	d_{1-14}=1.89	d_{2-9}=2.18	d_{2-10}=1.90	d_{3-10}=1.90
		d_{3-12}=2.15	d_{4-13}=2.15	d_{4-14}=1.90	d_{5-10}=2.05	d_{5-14}=2.06
		d_{6-10}=2.14	d_{6-11}=1.71	d_{7-11}=1.73	d_{7-14}=2.07	d_{8-9}=1.39
		d_{12-13}=1.40				
Cu_8O_8	Cu_8O_8	d_{1-9}=1.94	d_{1-14}=1.97	d_{2-10}=1.95	d_{2-11}=1.97	d_{3-11}=1.98
		d_{3-15}=1.93	d_{4-14}=1.96	d_{4-16}=1.93	d_{5-9}=1.99	d_{5-10}=2.06
		d_{5-15}=2.06	d_{5-16}=2.02	d_{6-11}=1.96	d_{6-14}=1.96	d_{7-11}=1.91
		d_{7-12}=1.94	d_{8-13}=1.94	d_{8-14}=1.92	d_{9-10}=1.55	d_{12-13}=1.40
		d_{15-16}=1.55				
	$Cu_8O_8^+$	d_{1-9}=2.08	d_{1-14}=1.93	d_{2-10}=2.07	d_{2-11}=1.94	d_{3-11}=1.94
		d_{3-15}=2.07	d_{4-14}=1.93	d_{4-16}=2.08	d_{5-10}=2.12	d_{5-15}=2.13
		d_{6-11}=1.92	d_{6-14}=1.93	d_{7-11}=1.95	d_{7-12}=1.82	d_{8-13}=1.83
		d_{8-14}=1.95	d_{9-10}=1.42	d_{12-13}=1.38	d_{15-16}=1.42	
	$Cu_8O_8^-$	d_{1-9}=1.92	d_{1-14}=1.95	d_{2-10}=1.84	d_{2-11}=1.97	d_{3-11}=1.95
		d_{3-15}=1.92	d_{4-14}=1.98	d_{4-16}=1.84	d_{5-9}=1.90	d_{5-15}=1.92
		d_{6-11}=1.98	d_{6-14}=1.95	d_{7-11}=1.91	d_{7-12}=2.13	d_{8-13}=2.15
		d_{8-14}=1.93	d_{9-10}=1.58	d_{12-13}=1.39	d_{15-16}=1.58	

J Phys Chem A. Author manuscript; available in PMC 2012 March 24.

Table 8

Average Cu-O-Cu angles in the copper oxide clusters using the B3LYP/LANL2DZ model chemistry

n	<Cu-O-Cu>
2	82
3	98
4	90
5	103
6	94
7	102